



## An experimental study on Fischer-Tropsch catalysis: Implications for impact phenomena and nebular chemistry

Yasuhito SEKINE<sup>1\*</sup>, Seiji SUGITA<sup>2</sup>, Takafumi SHIDO<sup>3</sup>, Takashi YAMAMOTO<sup>3</sup>,  
Yasuhiro IWASAWA<sup>3</sup>, Toshihiko KADONO<sup>4</sup>, and Takafumi MATSUI<sup>2</sup>

<sup>1</sup>Department of Earth and Planetary Science, Graduate School of Science, University of Tokyo,  
7-3-1 Hongo, Bunkyo-ku, Tokyo, 113-0033, Japan

<sup>2</sup>Department of Complexity Science and Engineering, Graduate School of Frontier Science, University of Tokyo,  
5-1-5 Kashiwanoha, Kashiwa, Chiba, 227-8562, Japan

<sup>3</sup>Department of Chemistry, Graduate School of Science, University of Tokyo, 7-3-1 Hongo, Bunkyo-ku, Tokyo, 113-0033, Japan

<sup>4</sup>Institute for Research on Earth Evolution, Japan Agency for Marine-Earth Science and Technology,  
2-15 Natsushima, Yokosuka, Kanagawa, 237-0061, Japan

\*Corresponding author. E-mail: [sekine@impact.k.u-tokyo.ac.jp](mailto:sekine@impact.k.u-tokyo.ac.jp)

(Received 05 April 2005; revision accepted 31 December 2005)

**Abstract**—Fischer-Tropsch catalysis, by which CO and H<sub>2</sub> are converted to CH<sub>4</sub> on the surface of transition metals, has been considered to be one of the most important chemical reactions in many planetary processes, such as the formation of the solar and circumplanetary nebulae, the expansion of vapor clouds induced by cometary impacts, and the atmospheric re-entry of vapor condensate due to asteroidal impacts. However, few quantitative experimental studies have been conducted for the catalytic reaction under conditions relevant to these planetary processes. In this study, we conduct Fischer-Tropsch catalytic experiments at low pressures ( $1.3 \times 10^{-4} \text{ bar} \leq P \leq 5.3 \times 10^{-1} \text{ bar}$ ) over a wide range of H<sub>2</sub>/CO ratios (0.25–1000) using pure iron, pure nickel, and iron-nickel alloys. We analyze what gas species are produced and measure the CH<sub>4</sub> formation rate. Our results indicate that the CH<sub>4</sub> formation rate for iron catalysts strongly depends on both pressure and the H<sub>2</sub>/CO ratio, and that nickel is a more efficient catalyst at lower pressures and lower H<sub>2</sub>/CO ratios. This difference in catalytic properties between iron and nickel may come from the reaction steps concerning disproportionation of CO, hydrogenation of surface carbon, and the poisoning of the catalyst. These results suggest that nickel is important in the atmospheric re-entry of impact condensate, while iron is efficient in circumplanetary subnebulae. Our results also indicate that previous numerical models of iron catalysis based on experimental data at 1 bar considerably overestimate CH<sub>4</sub> formation efficiency at lower pressures, such as the solar nebula and the atmospheric re-entry of impact condensate.

### INTRODUCTION

Fischer-Tropsch catalysis, by which CO and H<sub>2</sub> are converted to hydrocarbons, such as alkanes, alkenes, and alcohols, on the surface of transition metals, such as iron and nickel, has been suggested as playing a key role in abiotic organic synthesis under a variety of conditions in the solar system (e.g., Anders et al. 1973; Prinn and Fegley 1989; Kress and Tielens 2001; Hill and Nuth 2003; Sekine et al. 2003, 2005; Kress and McKay 2004). These conditions include the solar and circumplanetary nebulae, vapor clouds induced by impacts, and the atmospheric re-entry of vapor condensate due to asteroidal impacts. However, there are a number of problems in assessing the role of Fischer-Tropsch catalysis under these planetary conditions.

In the solar nebula chemistry, it has been suggested that the organic compounds in the carbonaceous chondrites might be produced by Fischer-Tropsch catalytic reaction (e.g., Studier et al. 1968; Anders et al. 1973; Hayatsu and Anders 1981; Bradley et al. 1984). However, it is still controversial whether the organics in meteorites are formed through Fischer-Tropsch catalysis in the solar nebula, because the experimental studies have shown that the isotopic fractionation patterns found in meteorites do not agree with those produced by Fischer-Tropsch catalysis (e.g., Cronin and Pizzarello 1990). Nevertheless, the important point is that Fischer-Tropsch catalysis would have been the only available thermally driven pathway to convert CO, which is energetically inhibited by the high activation barrier, into CH<sub>4</sub> in the solar nebula (Kress and Tielens 2001). Kress and

Tielens (2001) model Fischer-Tropsch reaction kinetics and apply it to the solar nebula conditions. Their results indicate that the present position of the asteroid belt may be the region where the Fischer-Tropsch catalysis occurs efficiently. More recently, several experiments were done under the conditions simulated for the nebula (e.g., Llorca and Casanova 1998, 2000; Fegley 1998; Llorca 1999; Ferrante et al. 2000; Hill and Nuth 2003). However, these measurements are not very quantitative. For example, the methane formation rate has not been measured. Recently, Sekine et al. (2005) conducted experiments under the condition of a circumplanetary subnebula and obtained the methane formation rate for metallic iron. Their result indicates that poisoning of the catalyst occurs even at very high  $H_2/CO$  ratios (e.g., 1000), and they apply the results to subnebula chemistry and the origin of methane on Titan. However, they use only iron as a catalyst. Under nebular conditions, nickel also exists as iron-nickel alloy. Although Llorca (1999) compares the difference between iron and kamacite in Fischer-Tropsch catalysis, the systematic study of the difference in catalytic efficiency among metallic iron, nickel, and iron-nickel alloy has not been conducted.

Fischer-Tropsch catalysis may also play an important role in asteroidal/cometary impacts on Earth and planets (Anders et al. 1973; Gerasimov et al. 2000; Sekine et al. 2003; Kress and McKay 2004). The impactor and a part of the target are vaporized upon impact of an asteroid/comet on a planet, and an impact vapor cloud is formed. Anders et al. (1973) suggest that catalytic reactions may occur on the surfaces of dust condensates in an expanding (and cooling) impact vapor cloud. In a cooling impact vapor cloud, gas-phase reactions are considered to quench around 2000 K (Fegley et al. 1986; Gerasimov et al. 1998). Around this temperature, the gas composition in the cloud is dominated by  $H_2$ , CO, and  $H_2O$ , which are generated by the dissociation of organics and water in meteorites and comets. At temperatures lower than 1000 K,  $CH_4$  becomes thermochemically more stable than CO (McKay and Borucki 1997; Kress and McKay 2004). However, gas-phase reactions proceed extremely inefficiently at such low temperatures. When heterogeneous catalysts such as iron and nickel condensates exist in the cloud,  $CH_4$  may be produced through heterogeneous catalytic reactions, such as Fischer-Tropsch catalysis (Kress and McKay 2004). Kress and McKay (2004) calculate the kinetics of the catalysis and assess the possibility of  $CH_4$  production in cometary impact vapors.

Furthermore, after the expansion of impact clouds, a large amount of condensate is launched from the impact point, disperses globally, and re-enters the atmosphere, where it can then react with gas in the planetary atmosphere. Sekine et al. (2003) calculate global methane production via Fischer-Tropsch catalysis on the surface of re-entering condensates by iron meteorite impacts on early Earth. The methane produced in these impact phenomena may play an important role not

only in the atmospheric evolution as a greenhouse effect gas (Sagan and Chyba 1997; Kress and McKay 2004), but also in the origin of life (Chyba and Sagan 1992).

In order to understand planetary processes such as nebular chemistry, impact vapor clouds, and the atmospheric re-entry of vapor condensates due to asteroidal impacts on early Earth, quantitative experimental data at lower pressures and over wide range of  $H_2/CO$  ratios need to be obtained, as described below in the next section of this paper. However, today's available quantitative data of Fischer-Tropsch catalysis have been obtained mainly in industrial chemistry (e.g., Vannice 1975; Krebs et al. 1979; Goodman et al. 1980). Since the productivities of the hydrocarbons are not very good at lower pressures, the laboratory data under conditions relevant to planetary processes have not been reported in industrial chemistry. Because of the absence of the experimental data under such reaction conditions, significant uncertainty remains in methane production via Fischer-Tropsch catalysis under planetary conditions (e.g., Kress and Tielens 2001; Sekine et al. 2003; Kress and McKay 2004). Thus, in this study, we conduct experiments on Fischer-Tropsch catalysis at lower pressures (<1 bar) and various  $H_2/CO$  ratios (0.25–1000) using three types of catalysts: metallic iron, nickel, and iron-nickel alloys. We compare iron and nickel catalysts under these reaction conditions and investigate the relation among pure iron, pure nickel, and iron-nickel alloys as catalysts.

In the next section, we first describe the experimental system of this study. Second, we show the results for the gas species produced via catalytic reactions and the methane formation rates for the catalysts. Next, we discuss the difference between iron and nickel and the mechanism of the reaction at lower pressures. Finally, we describe the implications for nebular chemistry and impact phenomena.

## EXPERIMENTAL

### Conditions

The pressure, temperature, and  $H_2/CO$  ratio are the main variables in this experiment. However, the relevant reaction temperature ranges only from 400 to 700 K (e.g., Krebs et al. 1979; Sekine et al. 2005), but pressure and the  $H_2/CO$  ratio vary widely in nebulae and impact vapor. Thus, pressure and the  $H_2/CO$  ratio become especially important in this study. In this section, we describe the pressure and the  $H_2/CO$  ratio under nebular conditions, cometary impact vapor, and the atmospheric re-entry of vapor condensate due to asteroidal impacts on early Earth.

Under solar and circumplanetary nebular conditions, the  $H_2/CO$  ratio is estimated to be very high (~1000–1500) because their compositions are expected to be similar to the hydrogen-rich solar abundance (Anders and Grevesse 1989). In the solar nebula, the gas pressure at catalytically optimal

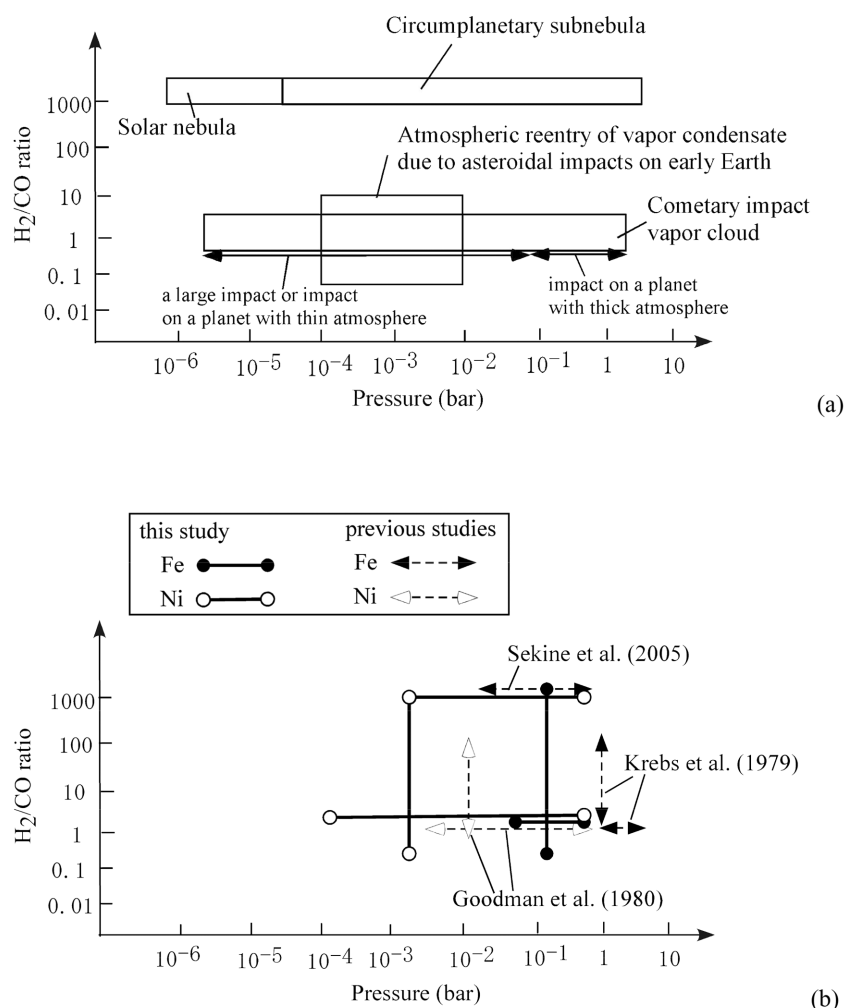


Fig. 1. a) Reaction conditions for Fischer-Tropsch catalysis in the solar nebula, a circumplanetary subnebula, cometary impact vapor clouds, and the atmospheric re-entry of vapor condensate due to asteroidal impacts on early Earth. b) The range of pressure and  $H_2/CO$  ratio of the previous experimental studies (broken lines) (Krebs et al. 1979; Goodman et al. 1980; Sekine et al. 2005) and that of this study for iron and nickel catalysts (solid lines).

temperatures ( $\sim 400$ – $700$  K) (Sekine et al. 2005) is estimated to be about  $10^{-6}$  to  $10^{-4}$  bar (e.g., Lewis and Prinn 1980; Bell et al. 1997, 2000). In a circumplanetary subnebula, gas pressure is estimated to be  $10^{-5}$  to 10 bar (e.g., Prinn and Fegley 1981; Coradini et al. 1989; Mousis et al. 2002; Mosqueira and Estrada 2003).

In cometary impact vapor, the abundance of CO at 2000 K (a typical quenching temperature of gas-phase reactions) is on the same order as that of  $H_2$  (McKay and Borucki 1997; Kress and McKay 2004). When a planet has a thick atmosphere, the expansion of the vapor cloud stops at the ambient atmospheric pressure, and the catalysis may proceed at relatively high pressures ( $\sim 1$  bar) (Kress and McKay 2004). However, when a planet has a thin atmosphere or an impactor is large enough to surpass a planetary atmosphere, the resulting vapor plume expands into space. Catalysis then takes place at very low pressures ( $\ll 1$  bar).

In the atmospheric re-entry of impact condensate, the reaction pressure ranges from  $\sim 10^{-4}$  to  $10^{-2}$  bar because the condensate reaches its slow terminal velocities at high altitudes of a planetary atmosphere (Sekine et al. 2003). A typical  $H_2/CO$  ratio is estimated to be 0.03–10 for early Earth's atmosphere (Sekine et al. 2003). Figure 1a shows the  $H_2/CO$  ratios and pressures estimated for nebular conditions, cometary impact vapor, and the atmospheric re-entry of impact condensate.

Figure 1b shows the range of pressure and  $H_2/CO$  ratio, for which the methane formation rate has been experimentally obtained for iron and nickel catalysts in the previous studies. In industrial chemistry, methane formation rates have been investigated experimentally at pressures higher than 1 bar and at  $H_2/CO = 4$ – $100$  for iron catalyst (Krebs et al. 1979) and at pressures higher than  $1.3 \times 10^{-3}$  bar and at  $H_2/CO = 4$  for nickel catalyst (Goodman et al. 1980). More recently, Sekine

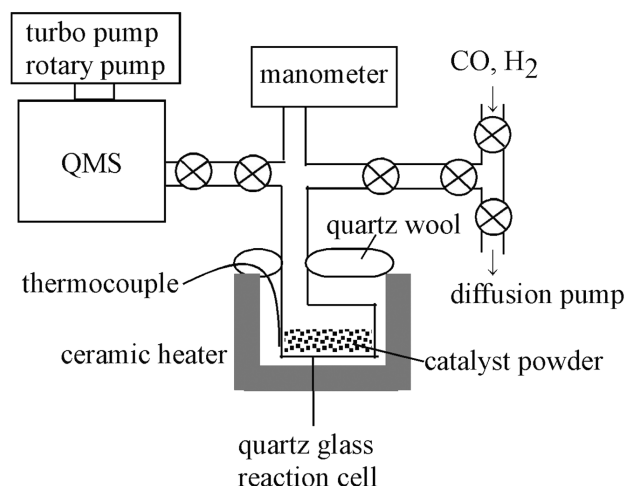


Fig. 2. A schematic diagram of the experimental system of Fischer-Tropsch catalysis, in which the gas mixtures are analyzed by a quadrupole mass spectrometer (QMS).

et al. (2005) obtained the methane formation rate for iron catalyst at  $\text{H}_2/\text{CO} = 1000$  and  $P = 2.0 \times 10^{-2} - 5.3 \times 10^{-1}$  bars. Thus, the range covered by the previous studies is much narrower than that needed for planetary applications.

In this study, we measure the methane formation rate and observe what gas species are formed as functions of pressure ( $1.3 \times 10^{-4}$  to  $5.3 \times 10^{-1}$  bars) and the  $\text{H}_2/\text{CO}$  ratio (0.25–1000) for both metallic iron and nickel catalysts. Figure 1b also shows the range of experimental conditions in this study. Our experimental conditions do not cover the entire reaction range, where the catalysis may occur in the solar nebula, impact vapor, and the atmospheric re-entry of impact condensate. However, our study extends the range of both the pressure and the  $\text{H}_2/\text{CO}$  ratio significantly.

### Catalysts

Under the conditions of the solar and circumplanetary nebulae, the impact vapor cloud, and the atmospheric re-entry of vapor condensate due to asteroidal impacts, iron and nickel may be the main catalysts in terms of Fischer-Tropsch reactions, because these elements are much more abundant metals in the solar nebula than other industrial Fischer-Tropsch catalysts, such as Ru and Co (Anders and Grevesse 1989). According to the estimates based on the C1-chondrite composition (Anders and Grevesse 1989), the  $\text{Fe}/\text{H}_2$  ratio is  $6.45 \times 10^{-5}$ , and the  $\text{Ni}/\text{H}_2$  ratio is about 1/20 times that of iron.

We use metallic iron, nickel, and iron-nickel alloy powders as catalysts because these catalysts may exist in a variety of planetary environments as small particles. The typical size of dust particles in the solar nebula and the condensate particles in impact vapors are estimated to be between sub-micron size to some hundreds of micrometer

(e.g., Prinn and Fegley 1989; Melosh 1982, 1989). The grain sizes of catalysts used in this study are  $\sim 250 \mu\text{m}$  for iron (Nilaco Corporation, 99.998% purity),  $\sim 63 \mu\text{m}$  for nickel (Nilaco Corporation, 99.9% purity), and  $\sim 40 \mu\text{m}$  for iron-nickel alloy (Koujundo-Kagaku Corporation, 99.9% purity) in diameter, respectively. The particle sizes of these catalysts are not exactly the same. However, according to Goodman et al. (1980), the size and shape of the catalyst do not affect the methane formation rate in Fischer-Tropsch catalysis significantly. We also use two types of iron-nickel alloy catalysts;  $\text{Fe:Ni} = 40:60$  (mol%) and  $\text{Fe:Ni} = 90:10$  (mol%).

In the following, we use a specific unit for a reaction rate: product molecules/site (= surface atoms)/s, in which the methane production rate (molecules/s) is normalized by the number of sites (i.e., surface atoms) of the catalysts. Thus, we need to measure the number of atoms (i.e., sites) on the surface of a catalyst. We measure the specific surface area ( $\text{m}^2/\text{g}$ ) for the catalysts with the Brunauer-Emmett-Teller (BET) method using Kr gas as the adsorbate for iron. As for the nickel and iron-nickel alloy catalysts, we estimate the specific surface area by measuring the pressure decrease caused by the adsorption of CO on the surface of the catalysts. The number of surface sites is estimated to be  $1.5 (\pm 0.1) \times 10^{18}$  site/g for the iron catalyst,  $1.6 (\pm 0.2) \times 10^{18}$  site/g for the nickel catalyst, and  $1.5 (\pm 0.2) \times 10^{17}$  site/g for the two iron-nickel alloys. The numbers of surface sites per unit weight for iron and nickel powders are close despite the difference in particle size. This is because the surfaces of the powder are not smooth but very irregular. The number of surface sites of the iron-nickel alloys is about 1/10 times that of the metallic iron and nickel. This is because the alloy powders have very smooth surfaces and an almost spherical shape.

### Experimental Systems

We constructed two experimental systems to measure Fischer-Tropsch catalytic reaction rates. Both systems are designed to be closed systems because low efficiency in the methane formation rate is expected at lower pressures. We use a gas chromatograph (GC) for one system, which is the same system used by Sekine et al. (2005). A schematic diagram is given in Fig. 1 by Sekine et al. (2005). We use a quadrupole mass spectrometer (QMS, MKS Instruments) for the other system. Figure 2 shows a schematic diagram of the experimental system using a QMS. A quartz reaction cell is located in a ceramic heater; the volume of the reaction cell is 155 ml. The powder of the catalysts is put in the reaction cell. A thermocouple, touching the reaction cell, is used to control the temperature. We used this system at reaction pressures lower than  $2.0 \times 10^{-2}$  bar because the GC is not suitable for experiments at such low pressures. The ratio of the number of surface sites of the catalysts to  $\text{H}_2$  molecule gas ( $\text{H}_2$  molecule/surface metal) in the systems varies about  $10^3$  to  $10^5$ , depending on reaction conditions.

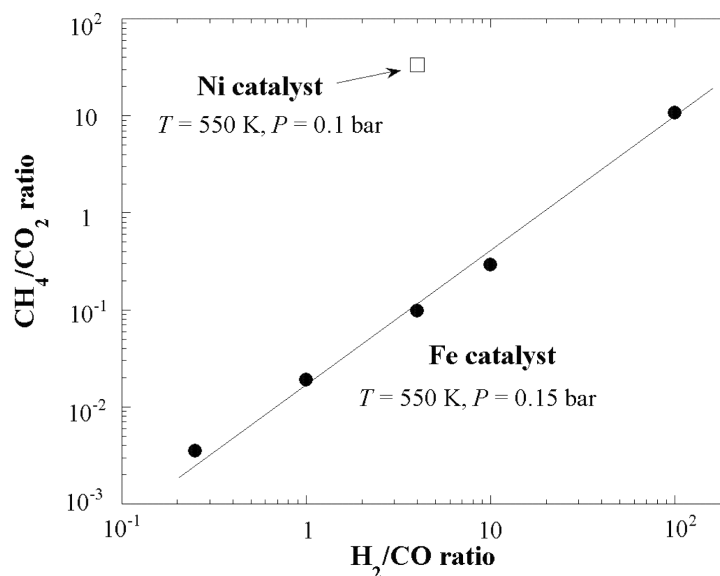


Fig. 3. The relationship between the production ratio of  $CH_4/CO_2$  as a function of the initial  $H_2/CO$  ratio for iron (solid circles) and nickel catalysts (open square) ( $H_2/CO = 4$ ,  $T = 550\text{ K}$ , and  $P = 0.15\text{ bar}$  for iron and  $P = 0.1\text{ bar}$  for nickel catalysts).

Because we followed the same experimental procedure used by Sekine et al. (2005), we describe it only briefly here. Prior to each measurement of reaction rate, the catalyst surface is cleaned with  $H_2$  gas at  $T = 700\text{ K}$  and  $P \sim 0.3\text{ bar}$  for 1.5 hr. This pre-treatment ensures that oxides of iron, nickel, and the alloys are reduced to metal before the main experiment. After the pre-treatment of the catalysts, we introduce reactant gas mixtures to the reaction cell. After a prescribed length of time, a part of the gas in the reaction cell is extracted and analyzed with the GC and the QMS. We analyze the gas mixtures after 5–9 different reaction times for each experimental condition. The methane production increases linearly with time under a given reaction condition (see Fig. 2 of Sekine et al. 2005). The gradient of the fit line gives the methane formation rates (molecules/site/s) under the reaction conditions. In our experiments, we measure the methane formation rates before 10% of the initial amounts of CO are consumed by surface reactions. When we conduct a reaction experiment at high temperatures ( $>600\text{ K}$ ), poisoning occurs. The poisoning is the gradual loss of catalytic activity by conversion of the surface carbide ( $C^*$ ) to unreactive graphitic carbon ( $G^*$ ) (e.g., Krebs et al. 1979). When the poisoning occurs on the surface of catalyst, the methane production decreases as reaction time. After equilibrium between  $C^*$  and  $G^*$  is achieved, the production rate approaches a steady state (e.g., Kress and Tielens 2001). In this study, we observed the poisoning at  $T = 625\text{ K}$  and  $P < 8.7 \times 10^{-4}\text{ bar}$  for the nickel catalyst and at  $T = 625\text{ K}$  and the entire range of pressure for the iron catalyst. When we observed the poisoning, we obtained the methane formation rate from the gradient of fitting line of methane production after the production proceeds in steady-state rate. This is

because almost all the Fischer-Tropsch reaction in the solar nebula and impact phenomena proceeds at this steady-state rate.

## RESULTS

In this section, we first compare the produced gas species between iron and nickel catalysts. Second, we compare the methane formation rates between the iron and the nickel catalysts as functions of  $H_2/CO$  ratio and pressure. The comparison reveals that there is a significant difference in catalytic properties between the iron and the nickel catalysts under planetary conditions. Third, we show the experimental results of the methane formation rate for the iron-nickel alloys and the relation among pure iron, pure nickel, and iron-nickel alloys at high and low  $H_2/CO$  ratios.

### Comparison between Iron and Nickel Catalysts

#### Gas Species

In our experiments,  $CH_4$ ,  $CO_2$ ,  $C_2H_6$ , and  $C_2H_4$  were observed as products of Fischer-Tropsch catalysis. In particular,  $CH_4$  and  $CO_2$  are the main products under the reaction conditions of this study. The production of  $CO_2$  at lower  $H_2/CO$  ratio can be explained by disproportionation of CO gas on the surface of the iron catalyst ( $2CO \rightarrow CO_2 + C^*$ ; Boudouard reaction) (e.g., Wentreck et al. 1976). Figure 3 shows the relationship between the production of  $CH_4/CO_2$  and  $H_2/CO$  ratio for iron catalyst at  $1.5 \times 10^{-1}\text{ bar}$  and 550 K and also the result for nickel catalyst at  $1.0 \times 10^{-1}\text{ bar}$  and 550 K. This result, shown in Fig. 3, suggests that  $CO_2$  production becomes predominant at low  $H_2/CO$  ratios for iron

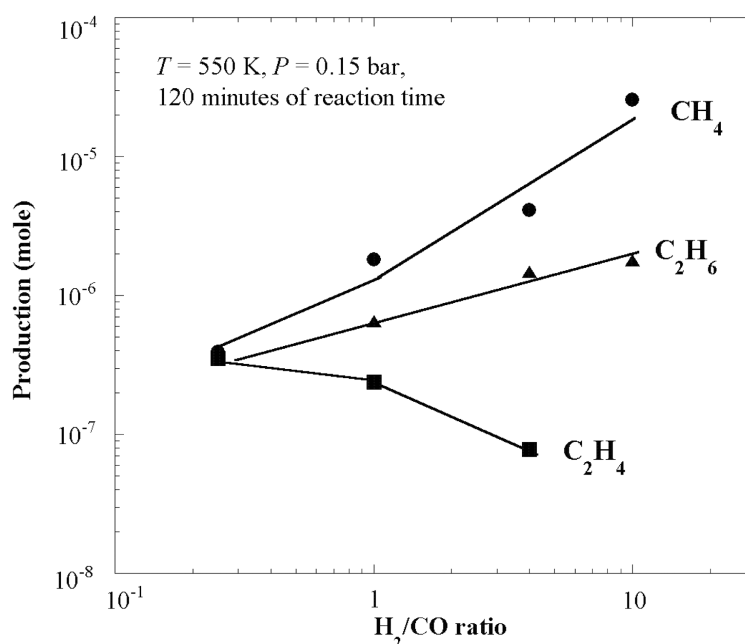


Fig. 4. The amount of hydrocarbons (CH<sub>4</sub> [circles], C<sub>2</sub>H<sub>4</sub> [squares], and C<sub>2</sub>H<sub>6</sub> [triangles]) produced using an iron catalyst as a function of H<sub>2</sub>/CO ratio ( $T = 550$  K,  $P = 0.15$  bar, and 120 min of reaction time).

catalyst under these reaction conditions, while CH<sub>4</sub> production is predominant for nickel catalyst. The production ratio of CH<sub>4</sub>/CO<sub>2</sub> for nickel catalyst is about 10<sup>3</sup> times that for iron catalyst at H<sub>2</sub>/CO = 4. The reason for this difference in the product gas species is described below in the “Difference between Iron and Nickel Catalysts” section.

Both C<sub>2</sub>H<sub>4</sub> and C<sub>2</sub>H<sub>6</sub> as well as methane are observed for iron catalyst. However, the production of C<sub>2</sub>H<sub>4</sub> and C<sub>2</sub>H<sub>6</sub> are not observed for nickel catalyst; almost exclusively methane is formed. This is consistent with the results of previous study of nickel catalyst in industrial chemistry at higher pressures (Goodman et al. 1980). Figure 4 shows the abundance of hydrocarbons produced on the surface of an iron catalyst as a function of H<sub>2</sub>/CO ratio. At lower H<sub>2</sub>/CO ratios (<1), the production of C<sub>2</sub>H<sub>4</sub> and C<sub>2</sub>H<sub>6</sub> becomes comparable to that of methane. Figure 4 also indicates that lower H<sub>2</sub>/CO ratios favor the formation of molecules with higher molecular weight for iron catalyst and also favor the formation of alkenes (such as C<sub>2</sub>H<sub>4</sub>) rather than that of alkanes (such as C<sub>2</sub>H<sub>6</sub>).

#### Methane Formation Rate

*The effect of the H<sub>2</sub>/CO ratio:* Methane formation rates for iron and nickel catalysts as functions of H<sub>2</sub>/CO ratio are shown in Fig. 5. We kept the pressure of reactant gas mixtures constant and changed the H<sub>2</sub>/CO ratio of reactant gas mixtures. The experiments were done at  $1.5 \times 10^{-1}$  bar and 550 K for iron and at  $2.0 \times 10^{-3}$  bar and 550 K for nickel catalyst. For nickel catalyst, methane formation rate increases

rapidly as the H<sub>2</sub>/CO ratio increases from 0.25 to 4, but shows little change at higher H<sub>2</sub>/CO ratios. Such a variation for nickel catalyst is reported for the methane formation rate on the (100) surface of nickel single crystal at  $1.3 \times 10^{-2}$  bar and 600 K (Goodman et al. 1980). Goodman et al. (1980) not only measured the methane formation rate but also observed the coverage of the surface carbon using Auger Electron Spectroscopy (AES). According to Goodman and coworkers (Goodman et al. 1980; Kelley and Goodman 1982), the methane formation rate is controlled by a delicate balance between carbon and hydrogen atoms adsorbed on the surface of the catalyst. At a given temperature, the concentration of surface hydrogen increases with hydrogen pressure until its saturation is achieved. Thus, the methane formation rate should increase with the concentration of hydrogen on the surface of the nickel catalyst. When the concentration of surface hydrogen reaches the saturation level, methane formation rate also reaches the maximum reaction rate. Further increase in the partial pressure of hydrogen in the reactant gas mixture leads to little change in methane formation rate. Thus, the data shown in Fig. 5 suggest that the surface hydrogen on the catalyst is saturated at H<sub>2</sub>/CO ratios higher than 4 under this reaction condition.

However, the increase in methane formation rate for an iron catalyst as a function of H<sub>2</sub>/CO ratio does not have a saturation point. Although there is no study observing the surface atom concentration similar to the case for nickel by Goodman et al. (1980), our results suggest that the hydrogen may not saturate on the surface of an iron catalyst even at a very high H<sub>2</sub>/CO ratio (e.g., 1000).

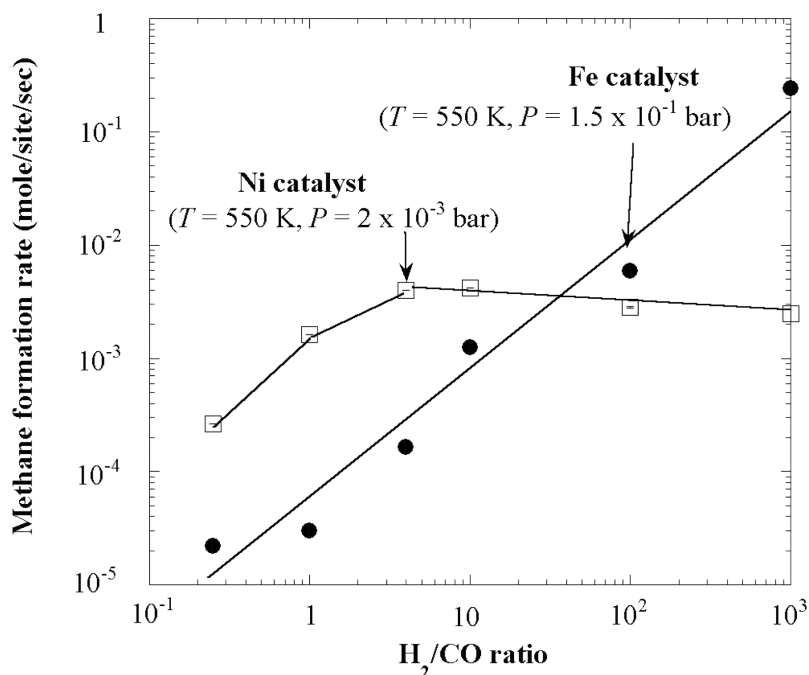


Fig. 5. Methane formation rates (molecules/site/s) for iron (solid circles) and nickel catalysts (open circles) as functions of  $H_2/CO$  ratio ( $T = 550$  K and  $P = 0.15$  bar for iron and  $P = 2.0 \times 10^{-3}$  bar for nickel).

*The effect of pressure:* Figures 6 and 7 show methane formation rates for iron and nickel catalysts as functions of pressure. Figure 6 compares the data for two different  $H_2/CO$  ratios. The lower  $H_2/CO$  ratio (i.e., 4) simulates the reaction conditions in a cometary impact vapor cloud and the atmospheric re-entry of vapor condensate due to asteroidal impacts on early Earth, while the higher value (i.e., 1000) simulates nebular conditions. Figure 7 compares the pressure dependence of the formation rate for iron and nickel catalysts. Our data for nickel at  $T = 500$  K and 625 K and  $H_2/CO = 4$  show good agreement with those of Goodman et al. (1980).

Figure 6 shows that the methane formation rate for iron catalyst strongly depends on the  $H_2/CO$  ratio, while that for nickel depends little on the  $H_2/CO$  ratio. Thus, at the higher  $H_2/CO$  ratio (i.e., 1000), iron is a more efficient catalyst for methane formation than nickel, but the nickel catalyst is a more efficient catalyst than iron at lower  $H_2/CO$  ratios.

Figure 7 shows that the iron catalyst depends more strongly on pressure than the nickel catalyst. For the nickel catalyst, poisoning is not observed in the entire pressure range from  $10^{-3}$ – $10^{-1}$  bar, and the methane formation rate at 625 K is higher than that at 500 K. However, for the iron catalyst, poisoning occurs at 625 K over the entire pressure range. We use the poisoned steady-state reaction rate of methane production as its formation rate for the iron catalyst at 625 K. Thus, the methane formation rate at 625 K is not significantly higher than that at 500 K. The trend shown in Fig. 7 indicates that iron is affected more by poisoning than nickel. For a nickel catalyst, the dependence on pressure becomes larger at higher temperatures (Goodman et al. 1980). In particular, the

methane formation rate for nickel depends little on pressure at 500 K. These experimental results indicate that the nickel catalyst becomes more important at lower pressures than the iron catalyst. Such a catalytic property is important in both solar nebula chemistry and the atmospheric re-entry of vapor condensate due to asteroidal impacts, because the reaction pressures of Fischer-Tropsch catalysis for these situations are much lower than 1 bar. The reason for this strong pressure dependence for the iron catalyst is also discussed in the “Difference between Iron and Nickel Catalysts” section below.

Figure 8 shows the methane formation rate for a nickel catalyst as a function of pressure at  $H_2/CO = 4$  and  $T = 625$  K. The gradient of the slope appears to be slightly larger at pressures lower than  $10^{-3}$  bar. The reason for this is discussed below in the “Poisoning” section.

### Iron-Nickel Alloy

In both solar and circumplanetary nebulae and in impact vapor clouds, metallic dust particles may not exist as pure iron or nickel but will be most likely to exist as iron-nickel alloys. Thus, the methane formation rate on the surfaces of iron-nickel alloys is very important. In this section, we show the methane formation rate for iron-nickel alloys and discuss the relationship among pure iron, pure nickel, and iron-nickel alloys in terms of catalytic methane formation efficiency.

Figure 9 shows the methane formation rate as a function of the molar iron ratio,  $Fe / (Fe + Ni)$ , in the catalyst at 500 K and 0.31 bars (Fig. 9a) and 0.16 bars (Fig. 9b). The data

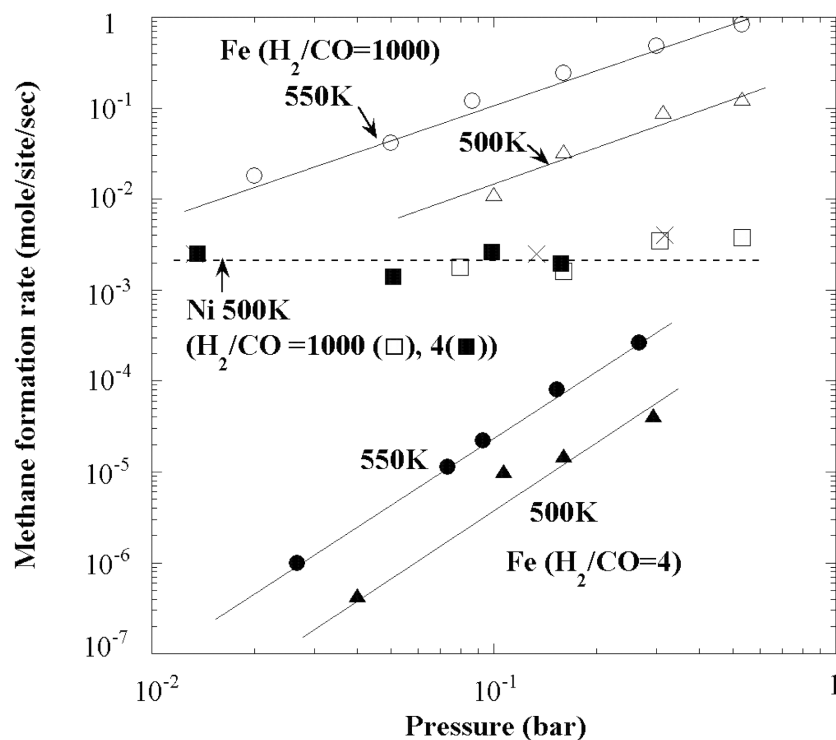


Fig. 6. Methane formation rate (molecules/site/s) as a function of pressure. Solid triangles and circles indicate results for an iron catalyst at  $H_2/CO = 4$ , and  $T = 500$  K and  $550$  K, respectively. Open triangles and circles indicate the previous results for an iron catalyst at  $H_2/CO = 1000$  and  $T = 500$  K and  $550$  K, respectively (Sekine et al. 2005). Squares indicate results for a nickel catalyst at  $T = 500$  K for  $H_2/CO = 4$  (solid) and  $1000$  (open). Previous results for a nickel catalyst by Goodman et al. (1980) at  $T = 503$  K and  $H_2/CO = 4$  are also shown (crosses).

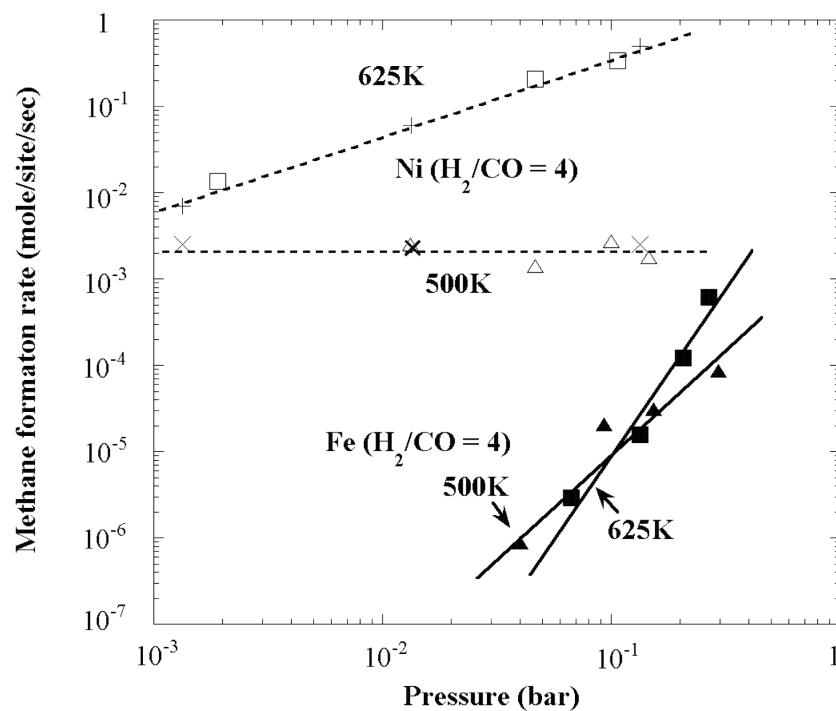


Fig. 7. A comparison of methane formation rate (molecules/site/s) as a function of pressure for an  $H_2/CO$  ratio of 4 between iron and nickel catalysts. Triangles are for iron (solid) and nickel (open) catalysts at  $T = 500$  K. Squares are for iron (solid) and nickel (open) catalysts at  $T = 625$  K. Previous results for a nickel catalyst at  $T = 503$  K and  $625$  K by Goodman et al. (1980) are also shown (crosses).



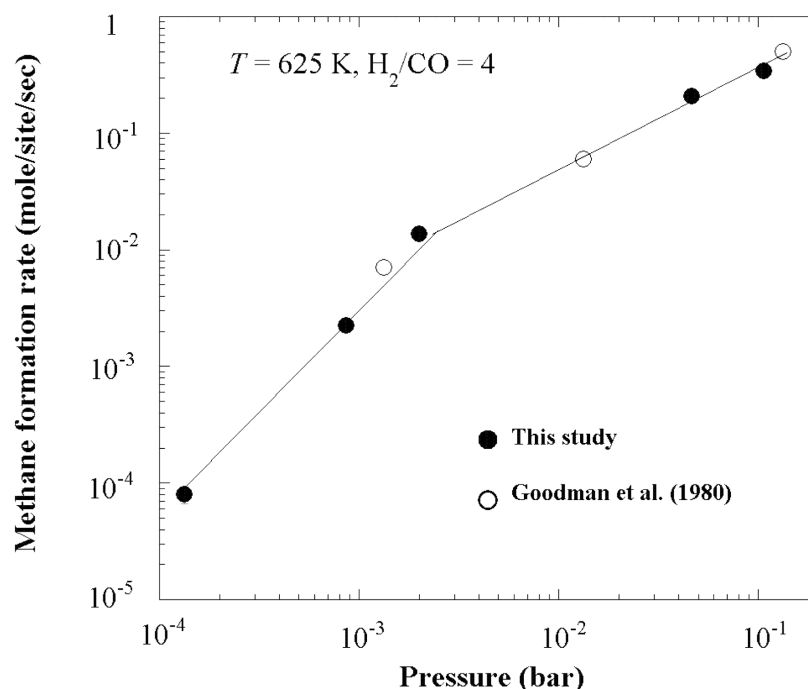


Fig. 8. Methane formation rate (molecules/site/s) for a nickel catalyst as a function of pressure ( $H_2/CO = 4$  and  $T = 625$  K). Solid and open circles are for data obtained in our study and those by Goodman et al. (1980), respectively.

shown in Fig. 9 indicate that the methane formation rate for iron-nickel alloys does not simply coincide with a linear interpolation of pure metals and that the real formation rate is lower than the linear interpolation line. However, it is important to note that methane formation rates for the alloys measured in this study are always between those for pure iron and pure nickel.

## DISCUSSION

### Difference between Iron and Nickel Catalysts

As shown in Fig. 3, the  $CH_4/CO_2$  ratio in the product of Fischer-Tropsch catalysis is different for iron and nickel catalysts.  $CH_4$  is the dominant product for the nickel catalyst, whereas  $CO_2$  is dominant for the iron catalyst at  $H_2/CO = 4$ . Figure 7 shows that the methane formation rate for an iron catalyst depends strongly on pressure, but such dependence is much smaller for a nickel catalyst.

These differences between iron and nickel catalysts may result from the difference in the rate of disproportionation of CO on iron and nickel catalysts. Hydrogenation of surface carbide ( $C^* + 4H^* \rightarrow CH_4$ ) removes carbides from surface sites and forms methane as a gas product. The disproportionation of CO ( $2CO \rightarrow CO_2 + C^*$ ) supplies surface carbides and forms  $CO_2$  as a gas product. Figure 10a shows a schematic diagram in which the disproportionation rate of CO (supply of carbide) is higher than the hydrogenation rate of  $C^*$  (removal of carbide) on the surface

of the catalyst. If this is the case, the concentration of surface carbide would be high and  $CO_2$  gas would be a dominant product. However, if the hydrogenation rate of  $C^*$  (removal of carbide) is higher than the disproportionation rate of CO (supply of carbide) on the surface of the catalyst (Fig. 10b), the main product will be methane and the concentration of surface carbon will be low. Our experimental data of gas products (Fig. 3) suggest that the catalytic reaction illustrated in Fig. 10a occurs more frequently on iron surfaces and that the reaction in Fig. 10b occurs more frequently on nickel surfaces.

According to AES observations of nickel catalysts by Goodman et al. (1980) and Kelley and Goodman (1982), a low concentration of surface nickel carbide induces efficient methane formation (see the "Methane Formation Rate" section). Jung and Thomson (1992) conduct dynamic X-ray diffraction observations of iron catalysts, which indicate that higher concentration of surface iron carbide induces lower catalytic activity for methane production. This is because the conversion of  $\epsilon'$ -iron carbide ( $Fe_{2.2}C$ ) to  $\chi$ -iron carbide ( $Fe_{2.5}C$ ) produces excess carbon on the surface ( $2.5Fe_{2.2}C \rightarrow 2.2Fe_{2.5}C + 0.3C$ ). These carbons prevent efficient methane formation and act as nucleation sites for further carbon deposition via Boudouard reaction ( $2CO \rightarrow CO_2 + C$ ). These previous studies are consistent with our discussion of the surface properties of iron and nickel catalysts illustrated in Fig. 10.

When the total pressure decreases, both the hydrogenation rate of  $C^*$  and the disproportionation rate of

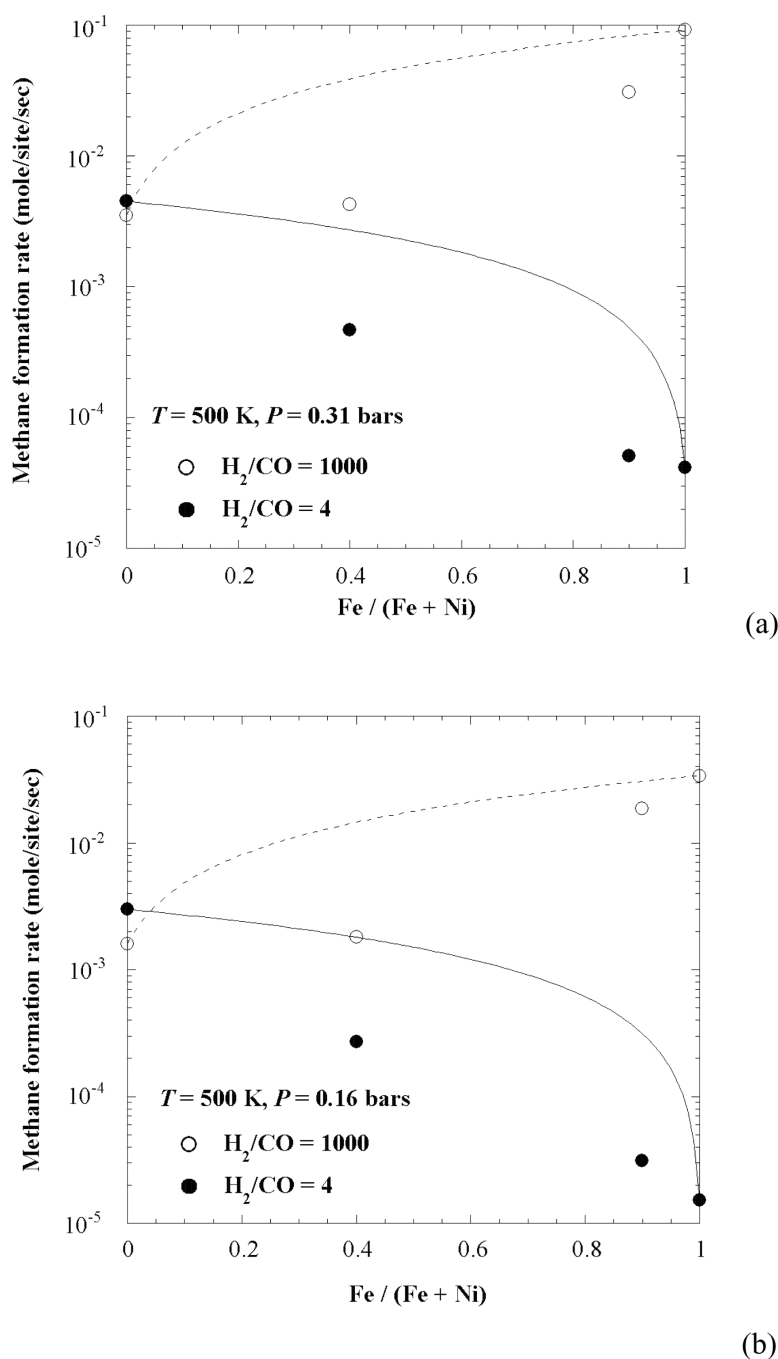


Fig. 9. Methane formation rate (molecules/site/s) as a function of the relative molar abundance of iron in an alloy catalyst ( $\text{Fe}/(\text{Fe} + \text{Ni})$ ) at 500 K. Two different pressures, 0.31 bars (a) and 0.16 bars (b), are used. The data at  $\text{Fe}/(\text{Fe} + \text{Ni}) = 0$  and 1 are for pure nickel and iron, respectively. The solid and broken curves are the linear combinations of the data of pure iron and nickel at  $\text{H}_2/\text{CO} = 4$  and 1000, respectively.

CO decrease. If the rate of decrease in the disproportionation rate of CO accompanying pressure decreases is lower than that of the hydrogenation rate of  $\text{C}^*$ , the concentration of the surface carbide becomes higher at lower pressures. In this case, the methane formation rate will become lower at lower pressures, because the increase in surface carbon leads to a decrease in the methane formation rate. If this is the case, then

the ratio of  $\text{CH}_4$  to  $\text{CO}_2$  will increase with pressure. Figure 11 shows the ratio of  $\text{CH}_4$  production to that of  $\text{CO}_2$  as a function of pressure. The results shown in Fig. 11 support the above hypothesis. The positive gradient observed in iron indicates that the ratio of  $\text{CO}_2$  to  $\text{CH}_4$  increases as pressure decreases. This result strongly suggests that the disproportionation of CO (supply of  $\text{C}^*$ ) proceeds more rapidly than the

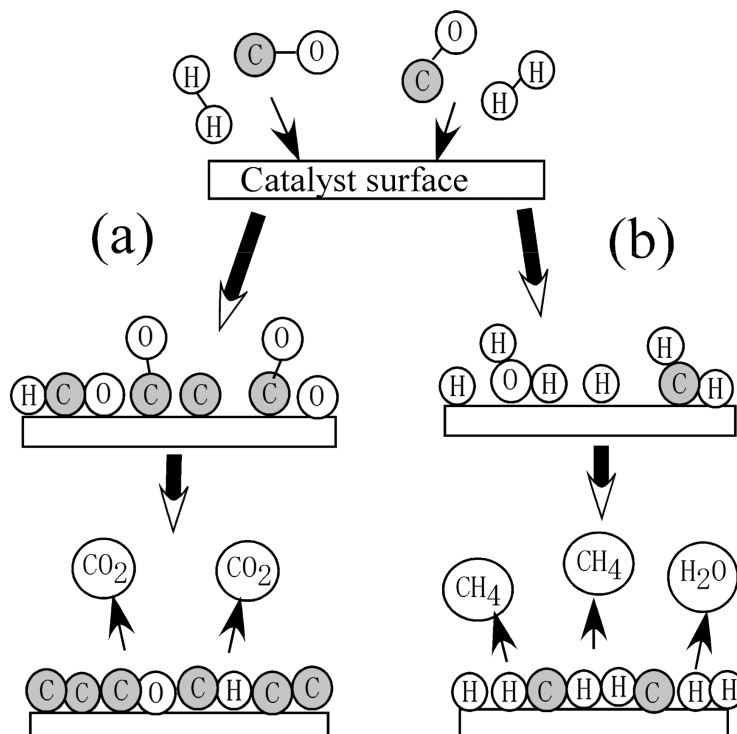


Fig. 10. A schematic diagram of the disproportionation of CO and the hydrogenation of C\* on the surface of catalysts. a) When the hydrogenation rate of C\* is lower than the disproportionation rate of CO, CO<sub>2</sub> becomes the dominant product and the surface is covered with carbon. b) When the hydrogenation rate of C\* is higher than the disproportionation rate of CO, CH<sub>4</sub> becomes the dominant product. The concentration of surface H also becomes high.

hydrogenation of C\* (removal of C\*) as the pressure decreases on the surface of the iron catalyst. This process might increase the concentration of surface carbon and lead to the observed low methane formation rate at lower pressures for the iron catalyst. In contrast, the CH<sub>4</sub>/CO<sub>2</sub> ratio for the nickel catalyst is higher at lower pressures. This suggests that the hydrogenation of C\* on the surface of the nickel catalyst proceeds rapidly at lower pressures. This may account for the observed high methane formation rates at lower pressures for the nickel catalyst.

### Poisoning

As shown in Fig. 8, we observed that the methane formation rate at 625 K for a nickel catalyst depends on pressure and that its dependence becomes slightly stronger at  $P \leq 10^{-3}$  bar. This may be due to the effect of poisoning of the catalyst. At pressures higher than  $1.3 \times 10^{-3}$  bar, the production rate is constant throughout the experimental time; no poisoning are observed for this reaction period. However, at  $1.3 \times 10^{-4}$  bar and  $8.7 \times 10^{-4}$  bar, the production rate of CH<sub>4</sub> decreases as reaction time increases; poisoning occurs. As described above in the “Methane Formation Rate” section, nickel is affected less by poisoning than iron. However, this result indicates that the poisoning tends to occur at lower pressures ( $P < 10^{-3}$  bar) and becomes an important reaction

step in estimating methane production even for the nickel catalyst.

The reason why the poisoning tends to occur at lower pressures may be explained as follows: At 625 K, methane formation rate decreases as pressure increases, as shown in Fig. 8. According to Kelley and Goodman (1982), a decrease in the methane formation rate is caused by an increase in the concentration of surface carbide. When the concentration of carbide increases and methane formation becomes inefficient, the residence time of surface carbide becomes long. This long residence time may permit carbide converting into graphitic carbon on the surface of the catalyst (i.e., poisoning). Although this hypothesis is promising, more detailed experimental studies on the characterization of the surface of catalysts, such as total organic carbon (TOC) analysis, transmission electron microscopy (TEM), and X-ray diffraction (XRD) measurements, are needed before a decisive conclusion is made.

## IMPLICATIONS FOR PLANETARY SCIENCE

### Nebular Chemistry

The reaction conditions in the solar nebula at the temperature range from 400 to 700 K, where Fischer-Tropsch catalysis takes place efficiently, are estimated to have H<sub>2</sub>/CO

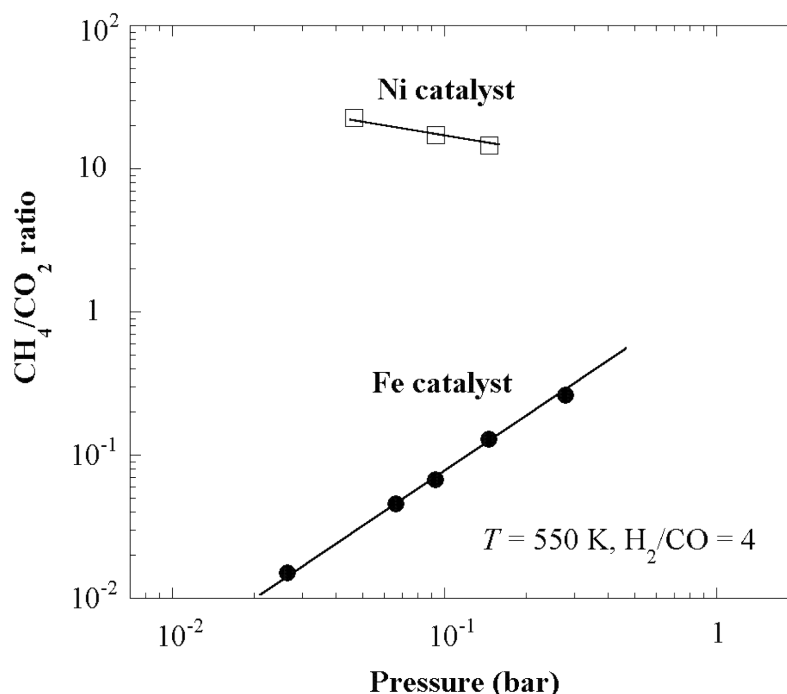


Fig. 11. The production ratios of  $\text{CH}_4/\text{CO}_2$  for iron (solid circles) and nickel catalysts (open circles) as functions of pressure ( $\text{H}_2/\text{CO} = 4$  and  $T = 550 \text{ K}$ ).

ratio ranging from 1000 to 1500 and pressure ranging from  $10^{-6}$  to  $10^{-4}$  bar (Anders and Grevesse 1989; Prinn 1993; Bell et al. 1997, 2000). Those for a circumplanetary subnebula are estimated to have similar  $\text{H}_2/\text{CO}$  ratios and pressures from  $10^{-5}$  to 10 bars (Prinn and Fegley 1981, 1989; Coradini et al. 1989; Mousis et al. 2002; Mosqueira and Estrada 2003). We did not conduct experiments under all of these conditions in this study because some conditions are out of the range covered by our experimental systems. However, some implications of Fischer-Tropsch catalysis for nebular chemistry may be predicted based on the results of our experiments.

As shown in Fig. 6, we observed that iron might be a more effective catalyst for methane formation via Fischer-Tropsch catalysis under the conditions of a circumplanetary subnebula (i.e., a high  $\text{H}_2/\text{CO}$  such as 1000) than nickel. Subnebula chemistry, including methane production by iron catalysts, is already discussed in our previous study (Sekine et al. 2005).

Under the conditions of the solar nebula (i.e., lower pressures), the results of our experiments cannot directly determine which metal is the main catalyst in the Fischer-Tropsch reaction, because the methane formation rate for an iron catalyst has a stronger pressure dependence than for a nickel catalyst (Figs. 6 and 7). It is difficult to conduct experiments under true solar nebula conditions, such as at very low pressures ( $10^{-6}$ – $10^{-5}$  bar) and long reaction times ( $10^{13}$  s, the life time of the solar nebula; see Prinn 1993).

For estimating methane production under the reaction

conditions beyond the parameter range in our experiments, model calculations of the kinetics of Fischer-Tropsch catalysis are useful (e.g., Kress and Tielens 2001). According to the numerical results by Kress and Tielens (2001), the methane formation rate for an iron catalyst is calculated to be  $\sim 10^{-1}$  molecules/site/s at  $P = 5 \times 10^{-4}$  bar,  $T = 500 \text{ K}$ , and  $\text{H}_2/\text{CO} \sim 1430$ . However, Fig. 6 indicates that the methane formation rate is  $\sim 10^{-2}$  molecules/site/s at  $P = 10^{-1}$  bar,  $T = 500 \text{ K}$ , and  $\text{H}_2/\text{CO} = 1000$ . This result strongly suggests that the methane formation rate at  $5 \times 10^{-4}$  bar, at which Kress and Tielens (2001) calculate the methane formation rate, should be much lower than the theoretical prediction by Kress and Tielens (2001) because of the strong pressure dependence of the iron catalyst. This discrepancy between numerical results and laboratory data is caused by the difference in catalytic properties between iron and nickel at lower pressures. As described in the introduction, the laboratory data on the methane formation rate for iron catalysts had not been obtained at lower pressures ( $< 1$  bar), while those for nickel catalysts have been investigated (Goodman et al. 1980). Kress and Tielens (2001) model the methane formation rate for iron catalysts via Fischer-Tropsch catalysis based on industrial data at 1 bar (Krebs et al. 1979) and calculate the methane formation rate for an iron catalyst at lower pressures with the assumption that the pressure dependence of iron catalysts is the same as for nickel. Thus, the numerical results for an iron catalyst by Kress and Tielens (2001) depend weakly on pressure; they considerably overestimate the rate of methane formation by iron catalysts in the solar nebula.

For a more accurate estimate of methane production in the solar nebula, we need to understand the series of reaction steps that control the entire reaction on the surface of catalysts and what determines the differences between iron and nickel catalysts. Our laboratory data suggest that the reaction steps involved in the disproportionation of CO, the hydrogenation of C\* and poisoning (see the "Discussion" section) determine the difference of catalytic properties between iron and nickel and are important for establishing the kinetic model of Fischer-Tropsch catalysis under planetary conditions. More laboratory data, such as in situ AES observations on the surface of individual iron catalysts, will be needed to develop such a kinetic model of Fischer-Tropsch catalysis.

### Impact Phenomena

As discussed in the introduction, Fischer-Tropsch catalysis may play a key role in chemical reactions occurring in expanding impact vapor clouds and in the atmospheric re-entry of vapor condensate due to asteroidal impacts on early Earth (Anders et al. 1973; Gerasimov et al. 2000; Sekine et al. 2003; Kress and McKay 2004). Under conditions that might occur during the atmospheric re-entry of impact vapor condensate on the early Earth ( $H_2/CO = 0.03\text{--}10$ ,  $P = 10^{-4}\text{--}10^{-2}$  bar) (Sekine et al. 2003), our experimental results suggest that metallic iron is not an effective catalyst because of its strong dependence on both pressure and  $H_2/CO$  ratio. These results reduce the methane production rate estimated by the theoretical calculation by Sekine et al. (2003), because their kinetic model is also based on the results of methane formation for an iron catalyst at 1 bar as Kress and Tielens (2001). However, when nickel exists in the impact phenomena as iron-nickel alloy and/or as pure nickel metal, then the methane formation rate does not decrease as drastically as for a pure iron catalyst. This is because the methane formation rate for nickel catalysts depends on pressure only very weakly at low  $H_2/CO$  ratio (Fig. 7). Figure 9 shows that the methane formation proceeds more efficiently on the surface of higher fraction of nickel in the iron-nickel alloy at  $H_2/CO = 4$ . This result strongly suggests that nickel may play an important role in the formation of methane in the atmospheric re-entry of impact vapor condensate.

Recently Hill and Nuth (2003) conducted Fischer-Tropsch catalytic experiments simulating the reaction in the solar nebula. They report that CN-bearing gas species, such as acetonitrile ( $CH_3CN$ ), were formed from  $H_2$ , CO, and  $N_2$  gas mixtures on the surfaces of iron silicate dust. Such production of CN-bearing gas species via Fischer-Tropsch catalysis also may have taken place during the atmospheric re-entry of impact condensate on the early Earth. Hashimoto and Abe (1995) calculate the atmospheric composition of Earth in the accretion stage, which indicates that a hydrogen-rich atmosphere has been formed. Recently, Tian et al. (2005) re-estimated the escape rate of hydrogen from Earth's early

atmosphere. Their results indicate that the balance between the low hydrogen escape and volcanic outgassing could have maintained a hydrogen mixing ratio of more than 30%. These studies suggest that  $H_2$  may have been one of the main gas species of Earth's early atmosphere, in addition to  $N_2$ ,  $CO_2$ , and CO proposed by previous photochemical model (e.g., Kasting 1990). In order to assess more precisely the role of the condensate during the re-entry process as a source of prebiotic molecules important for the origin of life, however, we need to conduct experiments with initial gas mixtures containing  $N_2$  and measure the formation rate of CN-bonded and other gas products on the surfaces of iron-nickel alloy particles at lower pressures.

In cometary impacts onto planets/satellites with thick atmospheres (Kress and McKay 2004), the catalysis will occur at relatively high pressures ( $\sim 1$  bar) compared to that for atmospheric re-entry of impact condensate. Under such conditions, both iron and nickel catalysts are efficient in promoting the Fischer-Tropsch reaction (Fig. 7). The  $H_2/CO$  ratio in cometary impact vapor is estimated to be low (i.e.,  $\sim 1\text{--}10$ ) (Kress and McKay 2004). Our experimental data in Fig. 4 show that the production of higher hydrocarbon, such as  $C_2H_4$  and  $C_2H_6$ , becomes comparable to the methane production at lower  $H_2/CO$  ratio. Since such higher hydrocarbons may have played an important role in the abiotic Earth after an impact, the formation rate of such higher hydrocarbons need to be studied more extensively as well.

### SUMMARY

We measured the methane formation rate and analyzed the gas products via Fischer-Tropsch catalysis for iron and nickel catalysts. We compared the properties of these catalysts and investigated the relationship among pure iron, pure nickel, and iron-nickel alloys. We conducted experiments over a wide range of  $H_2/CO$  ratio and pressures lower than 1 bar, where the data on Fischer-Tropsch catalysis is important in planetary science. We can summarize our experimental results as follows:

1. The production ratio of  $CH_4/CO_2$  is significantly different between iron and nickel catalysts. The  $CH_4/CO_2$  ratio in the products is much higher for nickel catalysts ( $CH_4$  dominant) than that for iron catalysts ( $CO_2$  dominant) at  $H_2/CO = 4$ .
2. The methane formation rate for iron catalysts increases monotonically with  $H_2/CO$  ratio, whereas that for nickel saturates at  $H_2/CO = 4$ .
3. The methane formation rate for iron catalysts depends more strongly on pressure than for nickel catalysts. The methane formation rate for iron catalysts drastically decreases as pressure decreases.
4. The reason for the strong pressure dependence of iron catalysts may be due to the change in concentration of

surface carbide produced by the disproportionation of CO. The disproportionation of CO on the surfaces of iron catalysts may proceed more rapidly than does the hydrogenation of surface carbide at lower pressures.

5. For nickel catalysts, no poisoning can be observed at higher pressures ( $P > 10^{-3}$  bar), but a significant rate of poisoning is observed at lower pressures.
6. The methane formation rate for iron-nickel alloy departs considerably from the linear interpolation line of data for pure iron and pure nickel metals, but is always found between the formation rates for pure iron and nickel catalysts.

Our experimental results suggest that the catalytic property of nickel becomes important under the reaction conditions formed in the atmospheric re-entry of vapor condensates due to asteroidal impacts on the early Earth, while iron is efficient in a circumplanetary subnebula. Under conditions with low  $H_2/CO$  ratios ( $<10$ ), such as in a cometary impact vapor cloud, our data also suggest that a large amount of  $C_2H_4$  and  $C_2H_6$  can be produced via Fischer-Tropsch catalysis. Thus, such larger hydrocarbons may be supplied to the prebiotic Earth due to impacts. Our data also suggest that the previous numerical studies (Kress and Tielens 2001; Sekine et al. 2003) overestimate the methane formation rate in the solar nebula and during the atmospheric re-entry of impact condensate. This is because the laboratory data concerning the methane formation rate for iron catalysts had not been obtained at lower pressures and they assumed that the pressure dependence for the methane formation rate for iron catalysts is same as that for nickel.

Our results suggest further that the three reaction steps concerning 1) the disproportionation rate of CO; 2) the hydrogenation rate of surface carbon; and 3) the poisoning rate of the catalyst determine the overall difference in the catalytic properties of iron and nickel. Furthermore, these three factors are important for establishing a kinetic model of Fischer-Tropsch catalysis under planetary conditions.

*Acknowledgments*—Y. Sekine thanks Takehiko Sasaki and Yoshimichi Namai for valuable discussions on the experiments. We greatly thank Joseph A. Nuth III and anonymous reviewer for their careful reviews and constructive comments. This research is partially supported by a Grant in Aid from Japan Society for the Promotion.

*Editorial Handling*—Dr. Scott Sanford

## REFERENCES

- Anders E. and Grevesse N. 1989. Abundances of the elements: Meteoritic and solar. *Geochimica et Cosmochimica Acta* 53:197–214.
- Anders E., Hayatsu R., and Studier M. H. 1973. Organic compounds in meteorites. *Science* 182:781–790.
- Bell K. R., Cassen P. M., Klahr H. H., and Henning T. 1997. The structure and appearance of protostellar accretion disks: Limits on disk flaring. *The Astrophysical Journal* 486:372–387.
- Bell K. R., Cassen P. M., Wasson J. T., and Woolum D. S. 2000. The FU Orionis phenomenon and solar nebula material. In *Protostars and planets IV*, edited by Mannings V. H., Boss A., and Russell S. Tucson, Arizona: The University of Arizona Press. 897 p.
- Bradley J. P., Brownlee D. E., and Fraundor P. 1984. Carbon compounds in interplanetary dust: Evidence for formation by heterogeneous catalysis. *Science* 223:56–58.
- Chyba C. F. and Sagan C. 1992. Endogenous production, exogenous delivery, and impact-shock synthesis of organic molecules: An inventory for the origin of life. *Nature* 355:125–132.
- Coradini A., Cerroni P., Magni G., and Federico C. 1989. Formation of the satellites of the outer solar system: Source of their atmospheres. In *Origin and evolution of planetary and satellite atmospheres*, edited by Atreya S. K., Pollack J. B., and Matthews M. S. Tucson, Arizona: The University of Arizona Press. pp. 723–762.
- Cronin J. R. and Pizzarello S. 1990. Aliphatic hydrocarbons of the Murchison meteorite. *Geochimica et Cosmochimica Acta* 54: 2859–2868.
- Fegley B. 1998. Iron grain catalyzed methane formation in the jovian protoplanetary subnebulae and the origin of the methane on Titan (abstract). *Bulletin of the American Astronomical Society* 30: 1092.
- Fegley M. B., Prinn R. G., Hartman G. H., and Watkins G. H. 1986. Chemical effects of large impacts on the Earth's primitive atmosphere. *Nature* 319:305–308.
- Ferrante R. F., Moore M. H., Nuth J. A. III, and Smith T. 2000. Laboratory studies of catalysis of CO to organics on grain analogs. *Icarus* 145:297–300.
- Gerasimov M. V., Dikov Y. P., Yakovlev O. I., and Wlotzka F. 2000. On the possibility of hydrocarbons synthesis during an impact (abstract #1259). 31st Lunar and Planetary Science Conference. CD-ROM.
- Gerasimov M. V., Ivanov B. A., Yakovlev O. I., and Dikov Y. P. 1998. Physics and chemistry of impacts. *Earth, Moon, and Planets* 80: 209–259.
- Goodman D. W., Kelley R. D., Madrey T. E., and White J. M. 1980. Measurement of carbide buildup and removal kinetics on Ni (100). *Journal of Catalysis* 63:226–234.
- Hayatsu R. and Anders E. 1981. Organic compounds in meteorites and their origins. *Topics in Current Chemistry* 99:1–37.
- Hashimoto G. L. and Abe Y. 1995. Chemical composition of early terrestrial atmosphere. Proceedings, 28th ISAS Lunar and Planetary Symposium. pp. 126–129.
- Hill H. G. M. and Nuth J. A. 2003. The catalytic potential of cosmic dust: Implications for prebiotic chemistry in the solar nebula and other planetary systems. *Astrobiology* 3:291–304.
- Jung H. and Thomson W. J. 1992. Dynamic X-ray diffraction study of an unsupported iron catalyst in Fischer-Tropsch synthesis. *Journal of Catalysis* 134:654–667.
- Kasting J. F. 1990. Bolide impacts and the oxidation state of carbon in the Earth's early atmosphere. *Origins of Life and Evolution of the Biosphere* 20:199–231.
- Kelley R. D. and Goodman D. W. 1982. Catalytic methanation over single crystal nickel and ruthenium: Reaction kinetics on different crystal planes and the correlations of surface carbide concentration with reaction rate. *Surface Science Letters* 123: L743–L749.
- Krebs H. J., Bonzel H. P., and Gafner G. 1979. A model study of the hydrogenation of CO over polycrystalline iron. *Surface Science Letters* 99:570–580.

- Kress M. E. and Tielens A. G. G. M. 2001. The role of Fischer-Tropsch catalysis in solar nebula chemistry. *Meteoritics & Planetary Science* 36:75–91.
- Kress M. E. and McKay C. P. 2004. Formation of methane in comet impacts: Implications for Earth, Mars, and Titan. *Icarus* 168: 475–483.
- Lewis J. S. and Prinn R. G. 1980. Kinetic inhibition of CO and N<sub>2</sub> reduction in the solar nebula. *The Astrophysical Journal* 238: 357–364.
- Llorca J. 1999. Hydrocarbon synthesis in cometary grains. *Physics and Chemistry of the Earth C* 24:591–595.
- Llorca J. and Casanova I. 1998. Formation of carbides and hydrocarbons in chondritic interplanetary dust particles: A laboratory study. *Meteoritics & Planetary Science* 33:243–251.
- Llorca J. and Casanova I. 2000. Reaction between H<sub>2</sub>, CO, and H<sub>2</sub>S over Fe, Ni metal in the solar nebula: Experimental evidence for the formation of sulfur-bearing organic molecules and sulfides. *Meteoritics & Planetary Science* 35:841–848.
- McKay C. P. and Borucki W. J. 1997. Organic synthesis in experimental impact shocks. *Science* 276:390–392.
- Melosh H. J. 1982. *The mechanics of large meteoroid impacts in the Earth's oceans*. Boulder, Colorado: The Geological Society of America. pp. 121–127.
- Melosh H. J. 1989. *Impact cratering: A geologic process*. New York: Oxford University Press. 256 p.
- Mosqueira I. and Estrada P. R. 2003. Formation of regular satellites of giant planets in an extended gaseous nebula I: Subnebula model and accretion of satellites. *Icarus* 163:198–231.
- Mousis O., Gautier D., and Bockelée-Morvan D. 2002. An evolutionary turbulent model of Saturn's subnebula: Implications for the origin of the atmosphere of Titan. *Icarus* 156:162–175.
- Prinn R. G. 1993. Chemistry and evolution of gaseous circumstellar disks. In *Protostars and planets III*, edited by Levy E. H. and Lunine J. I. Tucson, Arizona: The University of Arizona Press. pp. 1005–1030.
- Prinn R. G. and Fegley B., Jr. 1981. Kinetic inhibition of CO and N<sub>2</sub> reduction in circumplanetary nebula: Implications for satellite composition. *The Astrophysical Journal* 249:308–317.
- Prinn R. G. and Fegley B. 1989. Solar nebula chemistry: Origin of planetary, satellite, and cometary volatiles. In *Origin and evolution of planetary and satellite atmosphere*, edited by Atreya S. K., Pollack J. B., and Matthews M. S. Tucson, Arizona: The University of Arizona Press. pp. 78–136.
- Sagan C. and Chyba C. F. 1997. The early faint sun paradox: Organic shielding of ultraviolet-labile greenhouse gases. *Science* 276: 1217–1221.
- Sekine Y., Sugita S., Kadono T., and Matsui T. 2003. Methane production by large iron meteorites impacts on early Earth. *Journal of Geophysical Research* 108:6-1–6-11.
- Sekine Y., Sugita S., Shido T., Yamamoto T., Iwasawa Y., Kadono T., and Matsui T. 2005. The role of Fischer-Tropsch catalysis in the origin of methane-rich Titan. *Icarus* 178:154–164.
- Studier M. H., Hayatsu R., and Anders E. 1968. Origin of organic matter in early solar system—I. Hydrocarbons. *Geochimica et Cosmochimica Acta* 32:151–173.
- Tian F., Toon O. B., Pavlov A. A., and Sterck H. D. 2005. A hydrogen-rich early Earth atmosphere. *Science* 308:1014–1017.
- Vannice M. A. 1975. The catalytic synthesis of hydrocarbons from H<sub>2</sub>/CO mixtures over the Group VIII metals. *Journal of Catalysis* 37:449–473.
- Wentreck P. R., Wood B. J., and Wise H. J. 1976. The role of surface carbon in catalytic methanation. *Journal of Catalysis* 43:361–366.
-